PHILOSOPHICAL
TRANSACTIONS B

royalsocietypublishing.org/journal/rstb

Research

Managing populations after a disease outbreak: exploration of epidemiological consequences of managed host reintroduction following disease-driven host decline

Jorge Arroyo-Esquivel[1], Alyssa-Lois M. Gehman[2,3], Kenneth F. Collins[4] and Fabio Sanchez[5,6]

[1]California Department of Fish and Wildlife, Sacramento, CA 95605, USA
[2]Hakai Institute, Campbell River, British Columbia V9H, Canada
[3]The University of British Columbia, Vancouver, British Columbia V6T, Canada
[4]Unaffiliated Researcher, Seattle, Washington 98115, USA
[5]Mathematics, Universidad de Costa Rica, San Pedro 11501, Costa Rica
[6]Centro de Investigacion de Matematica Pura y Aplicada, San José 11501, Costa Rica

JA-E, 0000-0003-4399-954X; KFC, 0009-0004-5796-1723; FS, 0000-0002-5552-3672

Disease outbreaks in wild populations worldwide can result in widespread mortality within populations, with the recovery of individuals being rare. An example of this population is the sunflower sea star *Pycnopodia helianthioides* o to an unidentified disease known as sea star wasting disease. *Pycnopodia* down control of kelp grazers in rocky reefs across the Northeastern Pacific coast. This, combined with the massive declines in kelp coverage observed during the 2015–2016 marine heat wave observed in the Northeastern Pacific, has sparked an interest in reintroducing *Pycnopodia* individuals on the coast to potentially assist in the recovery of the populations. However, the epidemiological implications of reintroducing healthy sea stars into the wild populations are an under-explored question. This work explores this question using a dynamical population model of *Pycnopodia.* We also find. This analysis provides valuable information on timing and intensity for restoring *Pycnopodia* populations.

This article is part of the theme issue ‘Managing infectious marine diseases in wild populations’.

Cite this article: Arroyo-Esquivel J, Gehman A-LM, Collins KF, Sanchez F. 2026 Managing populations after a disease outbreak: exploration of epidemiological consequences of managed host reintroduction following disease-driven host decline. *Phil. Trans. R. Soc. B* **381**: 20240333.
https://doi.org/10.1098/rstb.2024.0333

Received: 4 March 2025
Accepted: 18 September 2025

One contribution of 16 to the theme issue ‘Managing infectious marine diseases in wild populations’.

Subject Areas:
ecology, theoretical biology

Keywords:
disease-driven mortality, *Pycnopodia helianthioides*, sea star wasting disease, reintroduction, age-stage model

Author for correspondence:
Jorge Arroyo-Esquivel
e-mail: arroyoesquiveljorge@gmail.com

1. Introduction

Disease-induced mortality can lead to significant decreases in the density of natural populations, increasing their risk of extinction [1]. One of the most studied examples is the mass mortality of amphibian populations worldwide caused by the fungal pathogen *Batrachochytrium dendrobatidis* [2,3]. Effectively managing a population heavily affected by disease-induced mortality presents several challenges and depends on the nature of transmission (frequency versus density-dependent), the recovery rates of infected individuals and the population densities of both infected and total individuals [4].

Disease mitigation can come at a range of times throughout an epidemic. In terrestrial mammal systems, high-cost interventions during an outbreak can work to contain an epidemic as it happens [5,6]. In marine systems, it often takes years to identify the causative agent of disease [7], making early interventions less feasible 8 from other natural populations or conservation breeding facilities [9 the population. Introducing new individuals may affect genetic diversity and could cause outbreeding depression in the population [10]. In addition, an

THE ROYAL SOCIETY
PUBLISHING

increase in host density can lead to a rise in disease prevalence, which would cause the contrary effect to the actual goal [11].

An example of a population of conservation interest where the reintroduction of healthy individuals has been considered is the sunflower sea star, *Pycnopodia helianthoides* [12,13]. Sunflower star populations have declined globally by 90% as a result of sea star wasting disease (SSWD intensified these outbreaks, contributing to the massive population declines observed in the Northeastern Pacific [12,14,15]. A causative agent for SSWD, *Vibrio pectenicida*, has recently been identified [16]. Transmission of *V. pectenicida* is by direct contact and through water exposure, and as seen in the field, *P. helianthoides* has extremely high mortality rates when exposed to this pathogen [16]. While heatwaves have been associated with increased SSWD prevalence and severity, mortality is primarily attributed to the disease itself rather than direct thermal stress [15,17], but see [18]. Particular interest in the recovery of sunflower sea star populations has been driven by its role as a predator of purple sea urchins (*Strongylocentrotus purpuratus* [19–21down control of purple sea urchins by sunflower sea stars has been identified as potentially one of the main drivers of kelp decline on the northern coast of California [22]. Furthermore, the reintroduction of the sunflower population could be key to a more resilient kelp forest after recovery [20,23]. The population declines of this species, as well as the ecological impacts of these declines, have led to the sunflower star being listed as critically endangered by the IUCN, recommended for listing as endangered by COSEWIC in Canada, and classified as threatened by NOAA in the USA [14,24].

Given the ecological impacts of the sunflower sea star population's demise, there is a strong interest in reintroducing individuals to the regions where the population has become functionally extinct [13]. Although significant progress has been made on the technical methodology of breeding individual sea stars [25], to our knowledge, no evaluation of the potential increase or reduction in disease prevalence provide the best possible chance of successful recovery.

In this paper, we evaluate the population effects of introducing healthy sea stars into a population using a simple age-stage model of the sunflower sea star population. The following section (§2) outlines the model and describes our analysis of it. Following it, in §3, we present how the population growth rate is affected by different introduction strategies, both from an ecological and an eco-evolutionary perspective. We finish this paper by discussing in §4 how these results can inform managers in future sunflower sea star reintroduction efforts.

2. Methods

(a) Modeling

Our age-stage model follows the abundance of a sea star population separated into three classes: juveniles J, adults A and infected I individuals. The model follows these abundances through seasons t, with $t = 0$ representing winter. A seasonally variable number of juveniles r_t is produced for the following season. Therefore, we assume that recruitment occurs constantly throughout the year. This coincides with the observations in both of our sites where recruits were observed throughout the year, as well as with classic studies that reported spawning seasons of December–January and March–July, with metamorphosis of larvae occurring anywhere between 90 and 146 days post-spawning [26]. A fraction α of juveniles matures into adults. A proportion μ_S of all healthy juveniles and adults experiences mortality at each season.

For infected individuals, we model the infection process by assuming a season-dependent proportion β_t of individuals becomes to the possibility of sea stars of different species infecting our model population [27], we assume this infection is frequency-dependent. Recovery of *Pycnopodia* from SSWD is rare, and thus, we assume that an infected sea star cannot return to a healthy state [28]. Finally, a proportion μ_I of those infected individuals experiences each season.

We incorporate two additional control parameters to model the effects of introducing healthy individuals. These parameters correspond to the introduction of healthy juveniles ρ_J and adults ρ_A. We assume these parameters are a proportion of healthy juvenile and adult densities, respectively, as a way to illustrate the intensities of restoration required relative to the actual population size.

In equation form, our model follows:

$$\begin{pmatrix} J_{t+1} \\ A_{t+1} \\ I_{t+1} \end{pmatrix} = \begin{pmatrix} (1-\alpha)(1-\mu_S)(1-\beta_t)+\rho_J & r_t & 0 \\ \alpha(1-\mu_S)(1-\beta_t) & (1-\mu_S)(1-\beta_t)+\rho_A & 0 \\ (1-\mu_S)\beta_t & (1-\mu_S)\beta_t & 1-\mu_I \end{pmatrix} \begin{pmatrix} J_t \\ A_t \\ I_t \end{pmatrix} \tag{2.1}$$

(b) Parameter estimation

We estimated our model parameters (table 1) using recruitment surveys from two regions in the Northeastern Pacific coast: Saratoga Beach (Island County, WA, USA) and the central coast of British Columbia, Canada.

The study site at Saratoga Beach was a sandy environment located at the seaward edge of an extensive eelgrass (*Zostera marina*) bed. Two sea star species (*Pisaster brevispinus, Pycnopodia helianthoides*) were present, and a third (*Luidia foliolata*) was rare. the spring of 2020, monthly surveys were conducted along depth contours in four sub-habitats: in and on the edge of the eelgrass bed, in an area of seasonal kelp (*Saccharina latissima* to 10 m (mean lower low water). Four 10×2 m transects were surveyed in each sub-habitat, for a total site area of 320 m^2. Every sea star (radius >0.5 cm) was counted, measured and assessed for SSWD. Additionally, the associated substrate and activity level for each *Pycnopodia* was recorded.

The study area in British Columbia included 165 sites, surveyed from 2013 to 2024 at a range of habitat types, including rocky reefs, seagrass habitats, soft sediments and kelp forests [29]. At each site, 30 × 2 m transects were surveyed, with 3–8 surveys per

Table 1. Parameters of equation (2.1) and their baseline values, including their range of values explored in the global sensitivity analysis.

parameter	description	fixed simulation value	range
	baseline recruitment proportion of juvenile sea stars	winter: 0.55 recruits/adult spring: 0.71 recruits/adult summer: 0.59 recruits/adult : 0.35 recruits/adult	[0, 1]
	baseline infection proportion of sea stars	n: 0 proportion/season : 0.2 proportion/season	[0, 1]
	baseline maturation proportion of sea stars	0.18 proportion/season	[0, 0.5]
	mortality proportion of healthy sea stars	0.005 proportion/season	[0, 0.05]
	mortality proportion of infected sea stars	0.95 proportion/season	[0.9, 1]

site. Sites are surveyed in May, July, August and October (although not evenly at all sites or all years). The depth range was between 0 and 10 m (Canadian Chart Datum; https://tides.gc.ca/en/vertical-datum-chart-references). Individuals were considered recruits when they were 2 cm size measured was 0.5 cm radius.

To get a generalized estimate of recruitment for the full region, we calculated the recruitment proportion at each season r_t by dividing the mean number of recruits observed in these sites at a given season by the number of adults observed. The infection proportion β was calculated using the line search algorithm by running the model with different values of β in order for the model to match the mean proportion of *Pycnopodia* detected with SSWD (approximately 15% for both sites; see [30]). Baseline maturation α was determined from the growth rate of juveniles calculated by [24] at approximately 8year. We then calculated α using this growth rate and the assumption that *Pycnopodia* reaches sexual maturity at a diameter of 11 cm (S. Gravem, personal communication, 2024). Mortality proportions of healthy and infected individuals were assumed to be extremely low and high, respectively.

(c) Data and model analysis

We analysed how a *Pycnopodia* population is affected by reintroduction efforts by estimating the population growth rate of model 1 using the baseline values provided in table 1. We start our simulations with an arbitrary initial population abundance N_0 where 25% of the population consists of juveniles, 74.25% consists of adults and 0.75% consists of infected individuals. Because the parameters of this model vary through time, we estimate the population growth rate λ using the geometric mean through time GM_t of the ratios of the season-over-season population abundances [31]. In equation form, this corresponds to:

$$\lambda = \mathrm{GM}_t\left(\frac{J_{t+1} + A_{t+1} + I_{t+1}}{J_t + A_t + I_t}\right). \tag{2.2}$$

We summarize parameter uncertainty by showing the mean of λ(line) and a 95% Monte Carlo quantile band, computed as the 2.5th–97.5th percentiles across 500 simulations with parameters drawn from the ranges in table 1. These bands reflect parameter uncertainty, not statistical confidence. It is worth noting that the arbitrary initial conditions determined in the previous paragraph do not affect the estimations of the population growth rate in this density-independent model [32].

We vary reintroduction efforts by timing (in what season reintroduction occurs) and intensity. We vary the intensity of reintroduction relative to the current abundance, i.e. an intensity of 10% corresponds to a reintroduction of several individuals that is equivalent to increasing the number of individuals of the corresponding age by 10%.

To evaluate the possibility of reintroduced individuals positively or negatively affecting the resistance to the disease, we test two scenarios: one where the proportion of individuals infected β_t is fixed and one where this proportion is reduced or increased to restoration efforts.

We perform a global sensitivity analysis (GSA) following the methods described in [33] to understand the relative importance of the different model parameters in the population growth rate. The GSA method uses the importance metric of a random forest trained on predicting the population growth rate under samples of the model parameters to identify which parameters are more important in determining such growth rate. The most critical parameters that determine the growth rate are identified using the importance metric of a random forest analysis, where a combination of different parameter values is used to predict the population growth rate. This metric is a relative measure of how much varying an individual parameter leads to a variation in the growth rate predicted by the trained random forest. We sample parameters from uniform distributions following the range for each parameter presented in table 1. In addition, we vary the intensity of reintroduction in the range of $0 - 50\%$ intensity, with 10% of parameter combinations having no reintroduction intensity. It is important to note that this analysis reflects the intrinsic sensitivities of the model and not the explained variance of the empirical data used to estimate the parameters in this model.

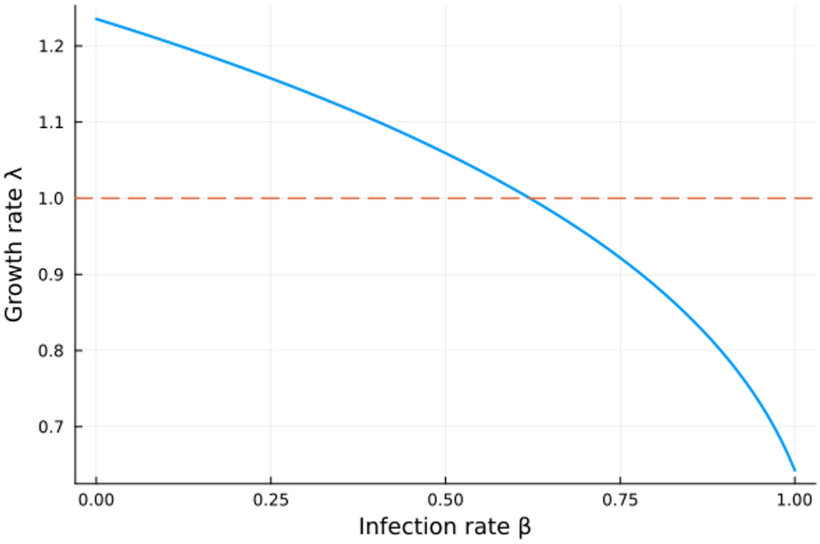

Figure 1. Population growth rate λ of model 1 as the proportion of infected individuals β varies. The horizontal line corresponds to $\lambda = 1$, which separates the parameter values whether a population grows ($\lambda > 1$) or decreases ($\lambda < 1$) in the long term.

3. Results

The relationship between population growth rate (λ) and infection rate (β) reveals a strong inverse correlation. As infection rates rise, population growth declines, and a critical threshold emerges where even small increases in β can drive long-term population decline. Figure 1 illustrates this trend, emphasizing the importance of disease management as a fundamental component of reintroduction efforts.

Moreover, our model suggests that the timing of seasonal events plays a crucial role in determining the success of reintroduction efforts. Modelled reintroductions conducted in spring and summer yield the highest population growth rates, particularly when juvenile reintroduction exceeds 30% of the current population (figure 2). This provides a framework for timing interventions to coincide with these favourable recruitment conditions that can enhance reintroduction success. Furthermore, our model indicates that while moderate-intensity reintroductions (20–30%) contribute significantly to population stability, there are diminishing returns beyond a certain threshold. Specifically, increases in λ become less pronounced beyond approximately 35% reintroduction intensity (figure 2). This threshold is further illustrated in figure 3, where the slope of the λ response curve flattens, indicating a reduced benefit per unit effort. This insight can guide managers towards more optimal allocation of limited conservation resources.

Reintroduction duration further influences population recovery. Our model results demonstrate that sustained efforts over multiple seasons lead to significantly higher long-term growth rates than short-term interventions. Even moderate reintroduction levels contribute to enhanced population resilience when maintained across several seasons, especially when reintroducing adult individuals (figure 4). Notice that an average increase in 0.5% 2% per year. This effect is particularly pronounced when reintroduction efforts reduce the prevalence of infection, as newly introduced healthy individuals dilute the proportion of infected individuals within the population. When increased reintroduction efforts increase the infection rate, we observe that the population growth rate still increases despite this increased infection rate. This is possibly caused by compensation for the reproduction events of the newly introduced adults. Figures 5 and 6 illustrate this effect, demonstrating the direct demographic support and epidemiological mitigation, which underscore the necessity of a long-term commitment to reintroduction programmes. It may not be feasible to have a long-term reintroduction programme lasting 25 years, but our results suggest that the longer the restoration effort can persist, the higher the impact it will have on population success.

GSA confirms that the infection rate (β) is the most influential factor affecting population growth in our model. This reinforces the need for targeted disease management strategies, such as minimizing contact rates between individuals in holding or release sites, identifying and using disease-free habitats for reintroduction or selectively breeding individuals with higher resistance to SSWD. Such actions aim to reduce the transmission rate and increase the probability of population persistence. This reinforces the need for targeted disease management in conjunction with reintroduction efforts. Additionally, the GSA results show that the maturation rate (α) and juvenile recruitment rate (r_t) also play important parts in determining λ, suggesting that promoting natural recruitment through improved larval survival conditions can further enhance recovery efforts. Figure 7 highlights the relative influence of key model parameters, with infection rate as the primary driver of population trends. The high impact of β in figure 7a suggests that in the absence of a decrease in infection prevalence, the reintroduction success remains limited. Conversely, figure 7b shows that when infection prevalence is mitigated through management strategies, reintroduction becomes far more effective. The high importance of the baseline infection rate in both graphics suggests that whether or not this infection rate is slightly affected by reintroduction efforts plays a small part in the overall population growth rate. This is a promising result that reduces the uncertainty in the risk of new infections produced by newly introduced individuals.

Our model suggests that targeted seasonal reintroductions in spring and summer have the potential to maximize recruitment success and resilience. Long-term reintroduction commitments yield better outcomes than short-term interventions, reinforcing the importance of sustained efforts. Disease management is crucial to success, as unchecked infection rates can undermine even the most aggressive reintroduction programmes.

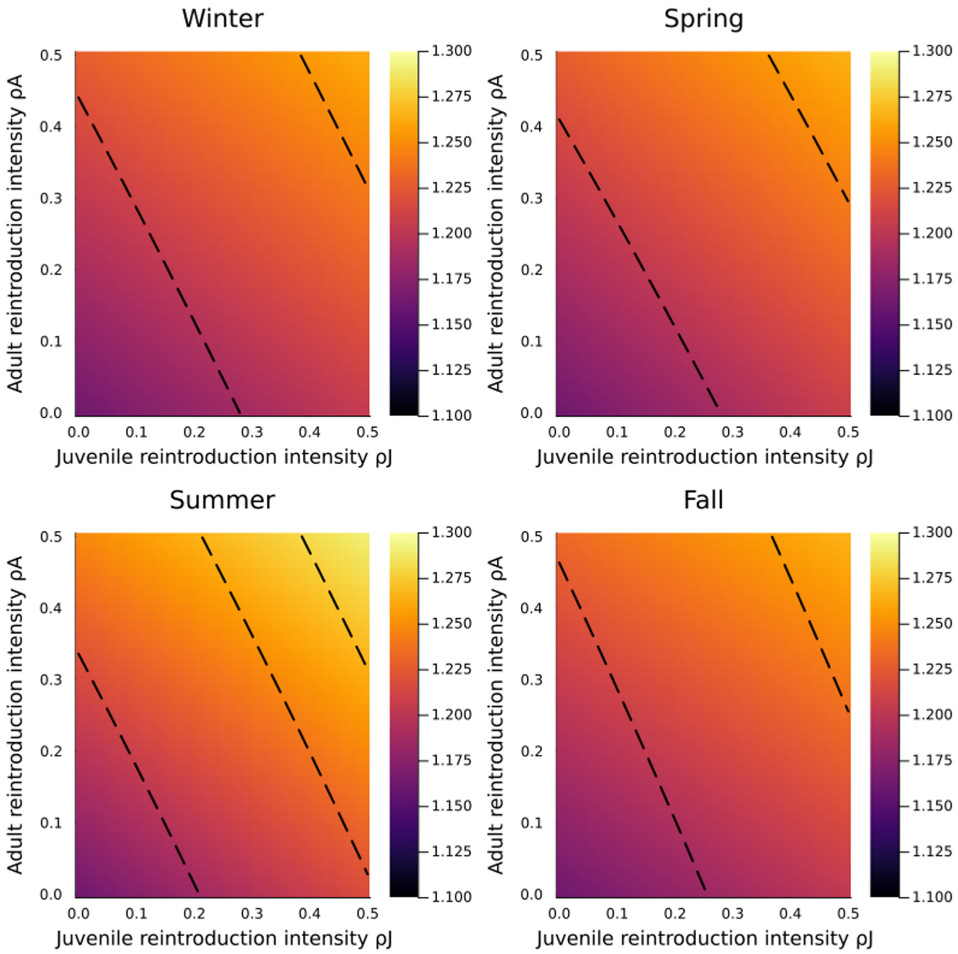

Figure 2. Population growth rate λ of model 1 at different reintroduction intensities (as percent of total abundance) of juvenile and adult individuals at different seasons. Black dashed lines represent isoclines from left to right of $\lambda = 1.2, 1.25, 1.275$.

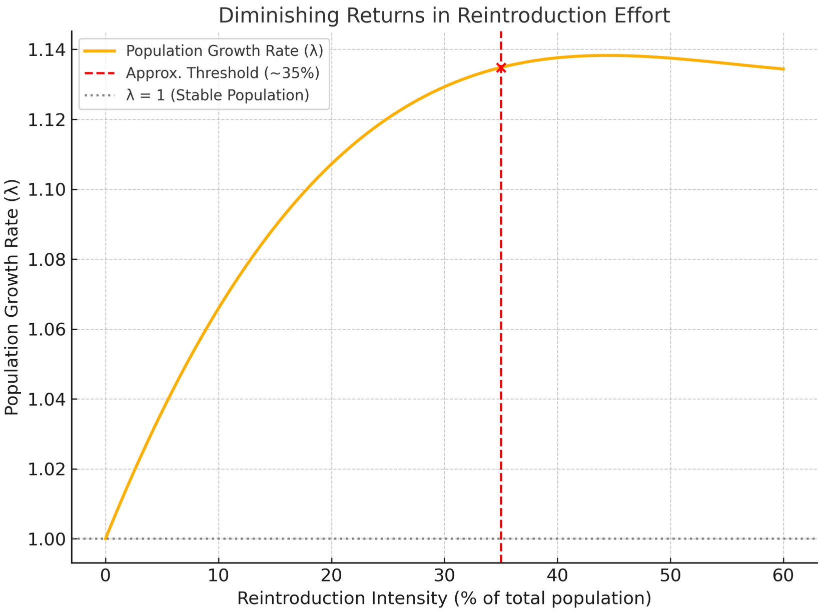

Figure 3. Population growth rate (λ) as a function of reintroduction intensity. The red dashed line indicates an approximate threshold (approx. 35%) beyond which additional reintroduction efforts yield diminishing returns.

To account for uncertainty in reintroduction intensity and duration, we simulated equation (2.1) for $T = 40$ seasonal steps (winter, spring, summer, autumn) with seasonal recruitment r_t (table 1) and infection occurring only in autumn (i.e. $\beta_t > 0$ in autumn; $\beta_t = 0$ otherwise). Introductions are modelled as proportional additions to the healthy classes at the release season (parameters ρ_J, ρ_A on the juvenile/adult diagonals of the projection matrix). We consider two schedules: (i) *summer-only*—releases occur only in summer and 'duration' counts the number of *consecutive summers* with releases (one release per summer); (ii) *all-seasons*—releases occur every season and 'duration' counts the number of *consecutive seasons* with releases starting in winter (one release per season).

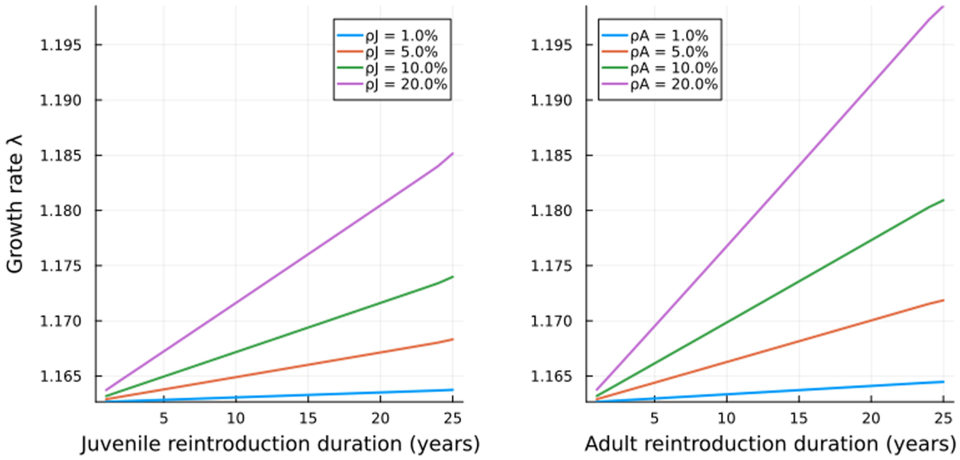

Figure 4. Population growth rate λ of model 1 at different summer reintroduction intensities of adults (as percent of total abundance) and durations if the proportion of infected individuals β does not change with the introduction of new individuals.

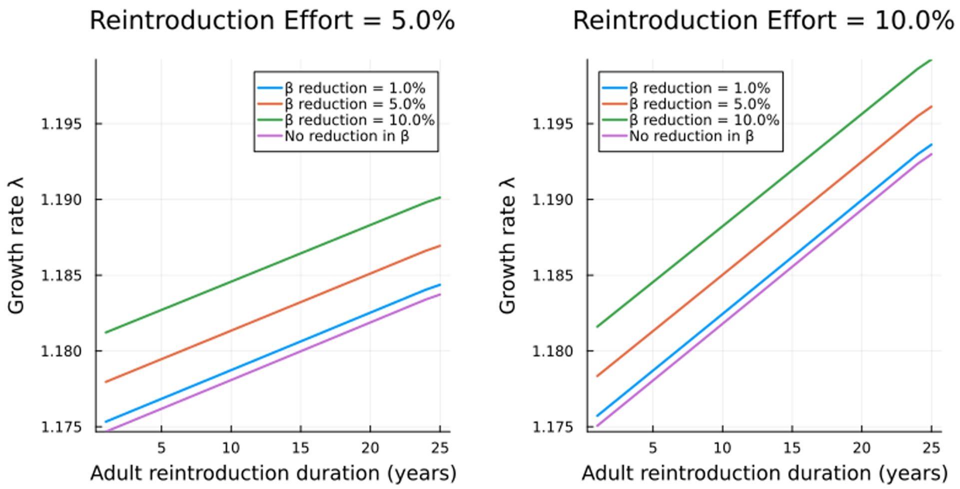

Figure 5. Population growth rate (λ) of model 1 at different summer reintroduction intensities (as percent of total abundance) and durations in the case that the proportion of infected individuals β decreases with the introduction of new individuals.

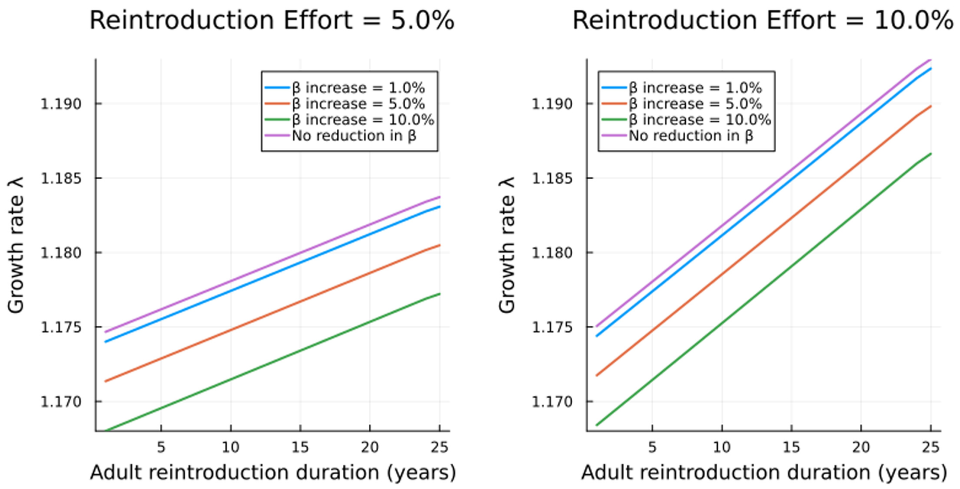

Figure 6. Population growth rate λ of model 1 at different summer reintroduction intensities (as percent of total abundance) and durations in the case that the proportion of infected individuals β increases with the introduction of new individuals.

Thus, for the all-seasons schedule, '10 seasons' means any 10 consecutive seasons (approx. 2.5 years), while for the summer-only schedule, '10' means 10 consecutive summers (approx. 10 years).

For each intensity–duration combination, we performed Monte Carlo simulations (parameters drawn uniformly within stated ranges in table 1; n draws per grid cell) and we report the mean λ across draws. To explicitly illustrate declining cases as requested by the referee, we also present a *conservative* parameter regime that expands the $\lambda < 1$ region (higher autumn infection, reduced recruitment and elevated healthy mortality): $\beta_{\text{fall}} \in [0.35, 0.60]$, a recruitment scaling factor in $[0.40, 0.70]$ applied to r_t,

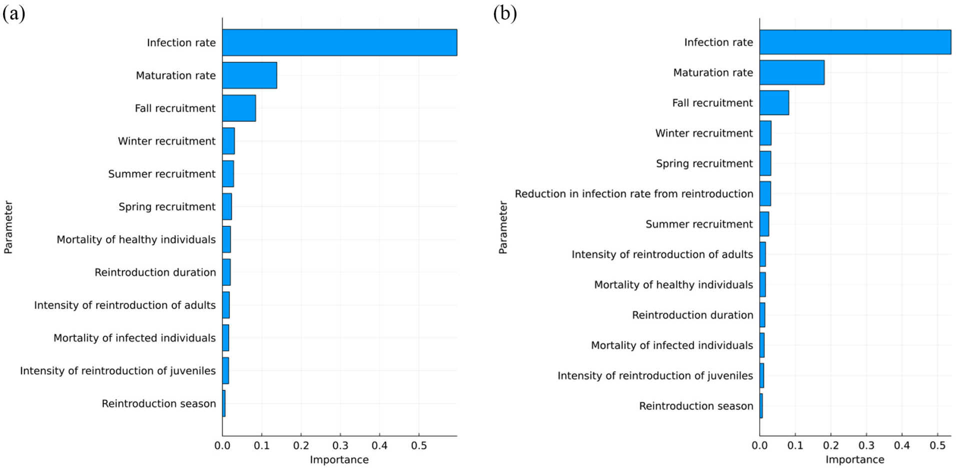

Figure 7. Relative importance of the different parameters to estimate the long-term growth rate λ of model 1 determined by the GSA (a) in the case where the proportion of infected individuals β does not change with the introduction of new individuals and (b) in the case the proportion of infected individuals β changes with the introduction of new individuals.

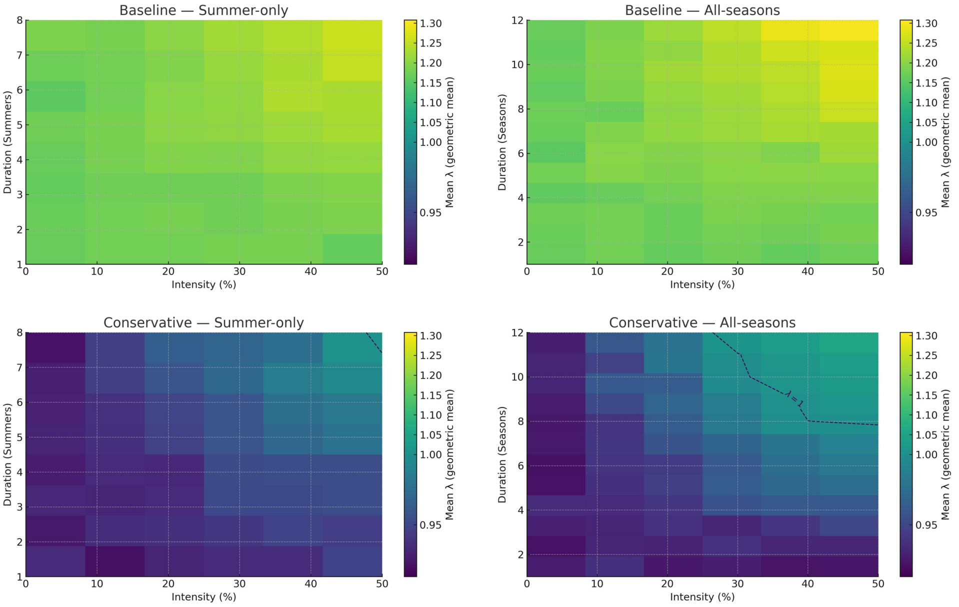

Figure 8. Mean population growth rate (λ) as a function of reintroduction intensity and duration under two schedules and two parameter regimes: baseline—summer-only, baseline—all-seasons, conservative—summer-only and conservative—all-seasons. Colours are centred at $\lambda = 1$; a dashed contour marks $\lambda = 1$ where the surface crosses that value. The conservative regime (higher fall infection, reduced recruitment, elevated healthy mortality) is included to explicitly display $\lambda < 1$ (declining) regions; see §2 for details.

$\mu_S \in [0.05, 0.10]$, with $\mu_I \in [0.95, 1]$ and $\alpha \in [0, 0.3]$. The heatmaps in figure 8 are centred at $\lambda = 1$ and include a dashed $\lambda = 1$ contour; values below the contour indicate long-term decline ($\lambda < 1$).

The resulting variation in λ is shown in figure 9. For the uncertainty panel (figure 9), we fixed the duration at five summers under the summer-only schedule and varied intensity. The uncertainty bands surrounding λ reflect realistic variation in ecological and epidemiological parameters. This high uncertainty reveals that even with high reintroduction intensities, the real long-term growth rate λ may still stay below 1. This observation motivates a more robust estimation of the parameters, especially those identified as most important by the GSA on figures 7.

4. Discussion

Our model findings provide critical insights into the reintroduction dynamics of *Pycnopodia* populations, revealing key interactions between infection rates, reintroduction strategies and long-term population viability. The results underscore the delicate balance between population growth and disease prevalence, demonstrating that the reintroduction efforts may fail to sustain viable populations without careful management. By analysing various scenarios, we identify strategic approaches that can maximize the effectiveness of conservation interventions.

This study identifies the primary drivers of population growth in a two-age-class model population affected by a disease without recovery. Our findings indicate that the disease's infection rate predominantly influences the population growth rate.

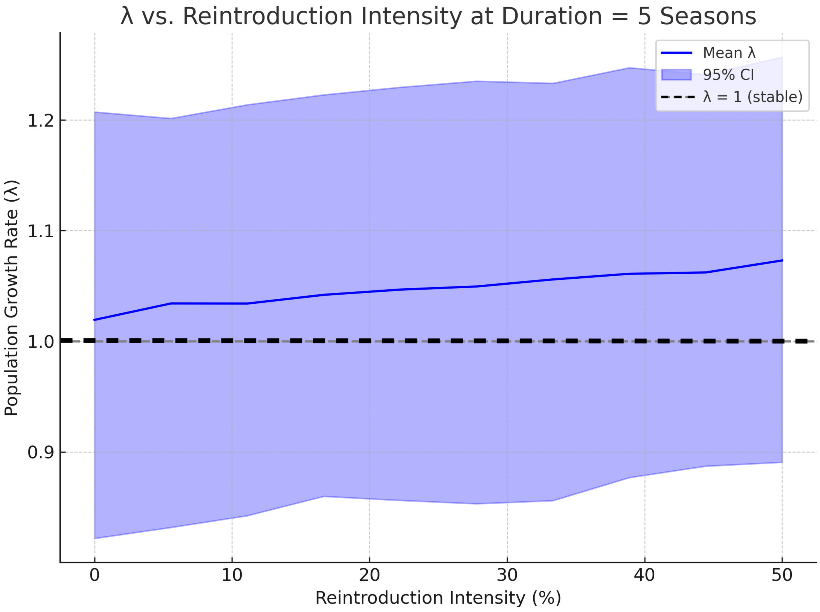

Figure 9. Long-term growth rate λ versus reintroduction intensity for *five summers* of releases (summer-only schedule) under the full matrix model equation (2.1). The line denotes the mean across 500 Monte Carlo parameter draws; the shaded band shows the 2.5th–97.5th percentiles with parameters sampled from the ranges in table 1. The dashed horizontal line marks $\lambda = 1$.

This result aligns with previous analyses, suggesting that high infection rates in a system with no recovery can prevent population persistence without external inputs [28]. Additionally, maturation rate exerts a smaller yet significant effect on population dynamics, consistent with findings in other marine organisms [34]. The growth rates observed in this analysis show the cases where infection is constant or only changes through reintroduction. In reality, temperature might play a part in driving infection rates [35,36]. Temperature can affect the dynamics by changing the infection rate as temperature varies [37]. Further studies on temperature dependence in SSWD would allow future models to incorporate these factors into their efforts.

In environments where the population can persist despite disease pressure, our results suggest that reintroduction efforts have a limited to moderate impact on population growth. However, our model indicates that this impact can be amplified by reintroducing adult individuals, particularly during the summer. A possible explanation for this outcome is that new adults introduced in the summer may compensate for those lost to infection in the subsequent autumn. While our model suggests that adult reintroduction exerts the most significant effect on population growth, there is a possible trade-off in time and resources between captive breeding juveniles and sexually mature adults. Additionally, empirical studies indicate that introducing individuals across multiple age classes can enhance the success of reintroduction efforts [11].

As expected, infection rates have a strong influence on the population response to reintroduction. However, the relatively low sensitivity of population growth to reintroduction intensity suggests that these results may be generalizable to sites where infection rates are high enough to prevent long-term persistence. In such cases, reintroduction efforts are probably most effective in areas where *Pycnopodia* has become functionally extinct owing to a population decline below a minimum viable population size and where the reintroduced individuals exhibit genetic resistance to the pathogen. Thus, breeding for genetic resistance for reintroduced individuals could expand the range of conditions wherein reintroduction efforts are successful.

Another key environmental factor influencing the population dynamics of *Pycnopodia* and other marine invertebrates is El Niño. The declines of *Pycnopodia* and other sea star populations over the past decade have been attributed to a combination of an intense El Niño event and a surge in SSWD [38]. Previous studies have linked these SSWD outbreaks to the elevated sea temperatures associated with El Niño and the marine heatwave of unprecedented duration in 1984 [17,39,40]. It is plausible that infection rates temporarily increase during these climatic events, leading to mass mortality and a subsequent decline in infection rates once the outbreak subsides. However, the precise mechanisms through which El Niño affects marine invertebrate population dynamics remain poorly understood. If temperature and disease are interacting, then heatwave conditions could potentially push populations to sufficiently high levels of disease transmission to keep the population growth rate low, despite high levels of introduction efforts previous to a heatwave. Improved knowledge of these interactions would facilitate the development of more accurate models for managing populations under El Niño conditions.

Beyond the omission of El Niño effects, our model also assumes that *Pycnopodia* recruitment occurs consistently each year and across all seasons, even at low population densities. While no direct evidence contradicts this assumption, data from Saratoga Beach, WA, indicate four recruitment events over the past 6 years, suggesting that recruitment may not occur yearly. The underlying drivers of this variability remain unknown, complicating efforts to incorporate irregular spawning into population models. If recruitment is episodic rather than continuous, we expect a reduction in population growth rates, potentially leading to population decline in specific sites. Under such conditions, the impact of reintroduction efforts would probably increase, as introducing healthy individuals could help to compensate for years or seasons with limited natural recruitment.

Finally, our model assumed that the dynamics of SSWD only affect a local, theoretical population of *Pycnopodia*. Dispersal of larvae can play a part in the infection dynamics of a *Pycnopodia* population by increasing the population growth rate through ecological rescue of populations with higher infection rates [28]. Accounting for dispersal may increase the population growth rate beyond what is presented in this article, especially in the case where fluid dynamics explicitly affect the dispersal to identify source and sink sites for larvae production [41]. This model has implicitly assumed the presence of other sea stars that affect these dynamics by considering the infection rate to be density-independent. Explicitly modelling these other sea star populations has the potential to further elucidate the dynamics of this disease and promote more holistic management practices to further reduce the infection rate in the target population [42].

In addition to the model limitations, a possible limitation of our analysis is the fact that long transient dynamics (long periods of perceived dynamic stability followed by a sudden transition into another, more stable state) may cause population declines to unsustainable levels before the long-term growth rate λ is reached by the population [43,44]. Previous models of populations with larval stages and infectious populations sensitive to long transients have shown that initial conditions can lead to quasi-stable conditions at which the population can present lower densities than predicted by the longer-term dynamics [45,46]. It is possible that some initial model conditions, especially when the infection rate is close to the critical threshold, may lead to longer-than-expected transients where the *Pycnopodia* population is low and may be susceptible to extinction by stochasticity [47]. Given that the parameter values estimated with our field surveys do not produce a long-term growth rate close to the threshold $\lambda = 1$, we suspect that these possible transients may not be long enough for these transients to present a risk for the *Pycnopodia* population.

This study highlights the complexity of post-disease population recovery and underscores the necessity of integrating epidemiological considerations into conservation planning. Our growth rate per season results can be used to evaluate the cost–benefit ratio for future management of marine systems, comparing recovery efforts aimed at *Pycnopodia* to those aimed at kelp recovery or sea urchin removal. In addition, the model introduced in this paper has the potential to be used or extended to assist in the understanding of disease dynamics for *Pycnopodia* and other sea star populations affected by SSWD. Future research should incorporate additional ecological drivers, such as climate variability and genetic resistance, to refine and optimize reintroduction strategies.

Ethics. This work did not require ethical approval from a human subject or animal welfare committee.

Data accessibility. Data used for estimating the parameters of this model are available at [48].

Declaration of AI use. We have not used AI-assisted technologies in creating this article.

Authors' contributions. J.A.-E.: conceptualization, formal analysis, investigation, methodology, project administration, software, supervision, writing—original draft, writing—review and editing; A.-L.M.G.: conceptualization, data curation, methodology, validation, writing—review and editing; K.F.C.: conceptualization, data curation, validation, writing—review and editing; F.S.: conceptualization, formal analysis, writing—review and editing.

All authors gave final approval for publication and agreed to be held accountable for the work performed therein.

Conflict of interest declaration. We declare we have no competing interests.

Funding. No funding has been received for this article.

References

1. McCallum H. 2012 Disease and the dynamics of extinction. *Phil. Trans. R. Soc. B* **367**, 2828–2839. (doi:10.1098/rstb.2012.0224)
2. Cheng TL, Rovito SM, Wake DB, Vredenburg VT. 2011 Coincident mass extirpation of neotropical amphibians with the emergence of the infectious fungal pathogen *Batrachochytrium dendrobatidis*. *Proc. Natl Acad. Sci. USA* **108**, 9502–9507. (doi:10.1073/pnas.1105538108)
3. Li Z, Wang Q, Sun K, Feng J. 2021 Prevalence of *Batrachochytrium dendrobatidis* in amphibians from 2000 to 2021: a global systematic review and meta-analysis. *Front. Vet. Sci* **8**, 1–13. (doi:10.3389/fvets.2021.791237)
4. Almberg ES, Manlove KR, Cassirer EF, Ramsey J, Carson K, Gude J, Plowright RK. 2021 Modelling management strategies for chronic disease in wildlife: predictions for the control of respiratory disease in bighorn sheep. *J. Appl. Ecol.* **59**, 693–703. (doi:10.1111/1365-2664.14084)
5. Acevedo-Whitehouse K. 2009 The importance of disease management programmes for wildlife conservation. *Anim. Conserv.* **12**, 185–186. (doi:10.1111/j.1469-1795.2009.00266.x)
6. Geret CP *et al*. 2011 Feline leukemia virus outbreak in the critically endangered Iberian lynx (*Lynx pardinus*): high-throughput sequencing of envelope variable region A and experimental transmission. *Arch. Virol.* **156**, 839–854. (doi:10.1007/s00705-011-0925-z)
7. Lafferty KD. 2025 Sea star wasting disease mystery finally solved. *Nat. Ecol. Evol.* **9**, 1552–1553. (doi:10.1038/s41559-025-02789-2)
8. Gravem Brown SA *et al*. 2026 Brace for the wave: planning for and responding to marine disease emergencies. *Phil. Trans. R. Soc. B* **381**, 20240332. (doi:10.1098/rstb.2024.0332)
9. Ebenhard T. 1995 Conservation breeding as a tool for saving animal species from extinction. *Trends Ecol. Evol.* **10**, 438–443. (doi:10.1016/s0169-5347(00)89176-4)
10. Fahselt D. 2007 Is transplanting an effective means of preserving vegetation? *Can. J. Bot.* **85**, 1007–1017. (doi:10.1139/B07-087)
11. Klop-Toker KL, Valdez JW, Stockwell MP, Fardell L, Clulow S, Clulow J, Mahony MJ. 2021 Improving breed-and-release programmes in the face of a threatening pathogen, *Batrachochytrium dendrobatidis*. *Aquat. Conserv. Mar. Freshw. Ecosyst.* **31**, 2788–2803. (doi:10.1002/aqc.3653)
12. Heady WN *et al*. 2021 Disease-driven mass mortality event leads to widespread extirpation and variable recovery potential of a marine predator across the eastern Pacific. *Proc. R. Soc. B* **288**, 20211195. (doi:10.1098/rspb.2021.1195)
13. Heady WN *et al*. 2022 *Roadmap to recovery for the sunflower sea star (Pycnopodia helianthoides) along the west coast of North America*. Sacramento, CA: The Nature Conservancy.
14. Gravem SA, Heady WN, Saccamonno VR, Alvstad KF, Gehman ALM, Frierson TN, Hamilton SL. *Pycnopodia helianthoides, sunflower seastar. IUCN Red List of Threatened Species 2021*. See https://www.iucn.nl/app/uploads/2021/03/red_list-2.pdf.
15. Harvell CD *et al*. 2019 Disease epidemic and a marine heat wave are associated with the continental-scale collapse of a pivotal predator (*Pycnopodia helianthoides*). *Sci. Adv.* **5**, eaau7042. (doi:10.1126/sciadv.aau7042)
16. Prentice MB *et al*. 2025 *Vibrio pectenicida* strain FHCF-3 is a causative agent of sea star wasting disease. *Nat. Ecol. Evol.* **9**, 1739–1751. (doi:10.1038/s41559-025-02797-2)
17. Eisenlord ME *et al*. 2016 Ochre star mortality during the 2014 wasting disease epizootic: role of population size structure and temperature. *Phil. Trans. R. Soc. B* **371**, 20150212. (doi:10.1098/rstb.2015.0212)

18. Menge BA, Cerny-Chipman EB, Johnson A, Sullivan J, Gravem S, Chan F. 2016 Sea star wasting disease in the keystone predator *Pisaster ochraceus* in Oregon: insights into differential population impacts, recovery, predation rate, and temperature effects from long-term research. *PLoS One* **11**, e0153994. (doi:10.1371/journal.pone.0153994)
19. Schultz JA, Cloutier RN, Côté IM. 2016 Evidence for a trophic cascade on rocky reefs following sea star mass mortality in British Columbia. *PeerJ* **4**, e1980. (doi:10.7717/peerj.1980)
20. Galloway AWE, Gravem SA, Kobelt JN, Heady WN, Okamoto DK, Sivitilli DM, Saccomanno VR, Hodin J, Whippo R. 2023 Sunflower sea star predation on urchins can facilitate kelp forest recovery. *Proc. R. Soc. B* **290**, 20221897. (doi:10.1098/rspb.2022.1897)
21. Whippo R, Gravem S, Porter-Hughes E, Galloway AWE. 2024 The sunflower sea star reduces grazing rates of purple sea urchins dependent upon urchin starvation state. *Ecosphere* **15**, e4948. (doi:10.1002/ecs2.4948)
22. Rogers-Bennett L, Catton CA. 2019 Marine heat wave and multiple stressors tip bull kelp forest to sea urchin barrens. *Sci. Rep.* **9**, 15050. (doi:10.1038/s41598-019-51114-y)
23. Arroyo-Esquivel J, Adams R, Gravem S, Whippo R, Randell Z, Hodin J, Galloway AWE, Gaylord B, Baskett ML. 2024 Multiple resiliency metrics reveal complementary drivers of ecosystem persistence: an application to kelp forest systems. *Ecology* **105**, e4453. (doi:10.1002/ecy.4453)
24. Lowry D *et al*. 2022 *Endangered species act status review report: sunflower sea star (Pycnopodia helianthioides): Final Report to the National Marine Fisheries Service, Office of Protected Resources*. Lacey, WA: National Marine Fisheries Service, Office of Protected Resources.
25. Hodin J, Pearson-Lund A, Anteau FP, Kitaeff P, Cefalu S. 2021 Progress toward complete life-cycle culturing of the endangered sunflower star, *Pycnopodia helianthoides*. *Biol. Bull.* **241**, 243–258. (doi:10.1086/716552)
26. Strathmann MF *et al*. 1987 *Reproduction and Development of Marine Invertebrates of the Northern Pacific Coast: Data and Methods for the Study of Eggs, Embryos, and Larvae*. Seattle, WA: University of Washington Press.
27. Kay SWC, Gehman ALM, Harley CDG. 2019 Reciprocal abundance shifts of the intertidal sea stars, *Evasterias troschelii* and *Pisaster ochraceus*, following sea star wasting disease. *Proc. R. Soc. B* **286**, 20182766. (doi:10.1098/rspb.2018.2766)
28. Calvo-Monge J, Arroyo-Esquivel J, Gehman A, Sanchez F. 2024 Source-sink dynamics in a two-patch si epidemic model with life stages and no recovery from infection. *Bull. Math. Biol.* **86**, 102. (doi:10.1007/s11538-024-01328-7)
29. Gehman ALM *et al*. 2025 Fjord oceanographic dynamics provide refuge for critically endangered *Pycnopodia helianthoides*. *Proc. R. Soc. B* **292**, 20242770. (doi:10.1098/rspb.2024.2770)
30. Nocedal J, Wright SJ. 2006 Line search methods. In *Numerical optimization*, pp. 30–65. New York, NY: Springer.
31. Logofet DO. 2013 Projection matrices in variable environments: λ_1 in theory and practice. *Ecol. Modell.* **251**, 307–311. (doi:10.1016/j.ecolmodel.2012.12.028)
32. Pick JB. 1997 Natural and spectral convergence measures of leslie matrices: additive norms and the imprimitive cases. *Math. Comput. Model*. **26**, 25–37. (doi:10.1016/S0895-7177(97)00167-2)
33. Harper EB, Stella JC, Fremier AK. 2011 Global sensitivity analysis for complex ecological models: a case study of riparian cottonwood population dynamics. *Ecol. Appl.* **21**, 1225–1240. (doi:10.1890/10-0506.1)
34. Denney NH, Jennings S, Reynolds JD. 2002 Life-history correlates of maximum population growth rates in marine fishes. *Proc. R. Soc. Lond. B* **269**, 2229–2237. (doi:10.1098/rspb.2002.2138)
35. Samuel GH, Adelman ZN, Myles KM. 2016 Temperature-dependent effects on the replication and transmission of arthropod-borne viruses in their insect hosts. *Curr. Opin. Insect Sci*. **16**, 108–113. (doi:10.1016/j.cois.2016.06.005)
36. Egilmez HI, Morozov AY, Clokie MRJ, Shan J, Letarov A, Galyov EE. 2018 Temperature-dependent virus lifecycle choices may reveal and predict facets of the biology of opportunistic pathogenic bacteria. *Sci. Rep.* **8**, 9642. (doi:10.1038/s41598-018-27716-3)
37. Ghosh S, Bhattacharyya S. 2007 Effect of temperature on viral infection and its control: a mathematical approach. *J. Theor. Biol.* **247**, 50–63. (doi:10.1016/j.jtbi.2007.02.009)
38. Marliave JB, Gibbs DM, Borden LA, Gibbs CJ. 2018 *Seabed biodiversity shifts identify climate regimes: the 2011 climate regime shift and associated cascades*. London, UK: InTech. (doi:10.5772/intechopen.71599)
39. Eckert GL, Engle JM, Kushner DJ. 2000 1999 Sea star disease and population declines at the channel islands. In *Proc. of the fifth California Islands symposium*. Washington, DC: U.S. Department of the Interior, Minerals Management Service. https://api.semanticscholar.org/CorpusID:210153011.
40. Bates AE, Hilton BJ, Harley CDG. 2009 Effects of temperature, season and locality on wasting disease in the keystone predatory sea star *Pisaster ochraceus*. *Dis. Aquat. Org.* **86**, 245–251. (doi:10.3354/dao02125)
41. Moreno Navas J, Telfer TC, Ross LG. 2011 Application of 3D hydrodynamic and particle tracking models for better environmental management of finfish culture. *Cont. Shelf Res*. **31**, 675–684. (doi:10.1016/j.csr.2011.01.001)
42. Portier J *et al*. 2019 Multi-host disease management: the why and the how to include wildlife. *BMC Vet. Res.* **15**, 295. (doi:10.1186/s12917-019-2030-6)
43. Abbott KC, Cuddington K, Hastings A. 2021 Transients in ecology: stochasticity, management, and understanding. *Theor. Ecol.* **14**, 623–624. (doi:10.1007/s12080-021-00524-8)
44. Francis TB, Abbott KC, Cuddington K, Gellner G, Hastings A, Lai YC, Morozov A, Petrovskii S, Zeeman ML. 2021 Management implications of long transients in ecological systems. *Nat. Ecol. Evol.* **5**, 285–294. (doi:10.1038/s41559-020-01365-0)
45. Arroyo-Esquivel J, Hastings A, Baskett ML. 2022 Characterizing long transients in consumer–resource systems with group defense and discrete reproductive pulses. *Bull. Math. Biol.* **84**, 102. (doi:10.1007/s11538-022-01059-7)
46. Bate AM, Hilker FM. 2013 Complex dynamics in an eco-epidemiological model. *Bull. Math. Biol.* **75**, 2059–2078. (doi:10.1007/s11538-013-9880-z)
47. Morozov A *et al*. 2020 Long transients in ecology: theory and applications. *Phys. Life Rev.* **32**, 1–40. (doi:10.1016/j.plrev.2019.09.004)
48. Gehman AL, Collins K. 2026 Data for parameter estimation of Managing populations after a disease outbreak: exploration of epidemiological consequences of managed host reintroduction following disease-driven host decline [Data set]. Zenodo. (doi:10.5281/zenodo.18599802)